

# A Circularly Permuted Photoactive Yellow Protein as a Scaffold for Photoswitch Design

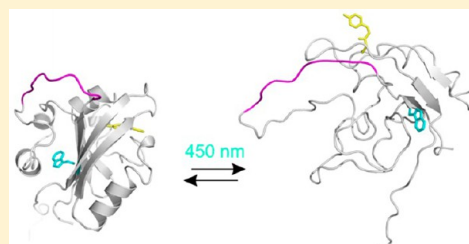
Anil Kumar,<sup>†</sup> Darcy C. Burns,<sup>†</sup> M. Sameer Al-Abdul-Wahid,<sup>‡</sup> and G. Andrew Woolley<sup>\*,†</sup>

<sup>†</sup>Department of Chemistry, University of Toronto, 80 St. George Street, Toronto, ON M5S 3H6, Canada

<sup>‡</sup>QANUC, 3420 University Street, McGill University, Montreal, QC H3A 2A7, Canada

## S Supporting Information

**ABSTRACT:** Upon blue light irradiation, photoactive yellow protein (PYP) undergoes a conformational change that involves large movements at the N-terminus of the protein. We reasoned that this conformational change might be used to control other protein or peptide sequences if these were introduced as linkers connecting the N- and C-termini of PYP in a circular permutant. For such a design strategy to succeed, the circularly permuted PYP (cPYP) would have to fold normally and undergo a photocycle similar to that of the wild-type protein. We created a test cPYP by connecting the N- and C-termini of wild-type PYP (wtPYP) with a GGSGGSGG linker polypeptide and introducing new N- and C-termini at G115 and S114, respectively. Biophysical analysis indicated that this cPYP adopts a dark-state conformation much like wtPYP and undergoes wtPYP-like photoisomerization driven by blue light. However, thermal recovery of dark-state cPYP is ~10-fold faster than that of wtPYP, so that very bright light is required to significantly populate the light state. Targeted mutations at M121E (M100 in wtPYP numbering) were found to enhance the light sensitivity substantially by lengthening the lifetime of the light state to ~10 min. Nuclear magnetic resonance (NMR), circular dichroism, and UV–vis analysis indicated that the M121E-cPYP mutant also adopts a dark-state structure like that of wtPYP, although protonated and deprotonated forms of the chromophore coexist, giving rise to a shoulder near 380 nm in the UV–vis absorption spectrum. Fluorine NMR studies with fluorotryptophan-labeled M121E-cPYP show that blue light drives large changes in conformational dynamics and leads to solvent exposure of Trp7 (Trp119 in wtPYP numbering), consistent with substantial rearrangement of the N-terminal cap structure. M121E-cPYP thus provides a scaffold that may allow a wider range of photoswitchable protein designs via replacement of the linker polypeptide with a target protein or peptide sequence.



Photoswitchable proteins offer the possibility for remote control of a variety of biochemical processes.<sup>1</sup> If one wishes to photocontrol the activity of a given target protein, a number of strategies may be envisaged. One design involves co-opting naturally occurring domains that undergo light-driven dimerization. Fusion of one domain to the target protein of interest and of its dimerization partner to a membrane localization sequence, for instance, can be used to effectively control the subcellular localization of the target.<sup>2,3</sup> A second strategy involves making hybrid proteins in which a photoswitchable domain is linked to a target protein in a manner that results in conformational changes in the photoreceptor being transferred to functional changes in the target.<sup>4–8</sup> As Möglich and Moffat have described in a review of engineered photoreceptors, this strategy is critically dependent on the nature on the linkage between the two proteins.<sup>9</sup>

The LOV domain has proven to be a workhorse for such engineering efforts; it has been thoroughly characterized by a range of structural methods and has the distinct advantage of having a naturally occurring cofactor.<sup>10–14</sup> Photoactive yellow protein (PYP) is another small water-soluble protein that undergoes blue light-driven photochemistry.<sup>15–18</sup> Although the PYP cofactor *p*-coumaric acid is not usually present except in specialized cell types, it can be added exogenously, or the

enzymes for its biosynthesis can be co-expressed with PYP.<sup>19</sup> From the point of view of designing novel photoswitchable bioactivity, PYP has a potential advantage in that it undergoes extensive conformational changes upon photoisomerization. These changes involve a large increase in protein internal dynamics and large-scale rearrangements and/or detachment of the N-terminal cap domain from the rest of the protein.<sup>17,20</sup> The conformational change of PYP has been engineered to photocontrol other proteins, in particular the GCN4 DNA binding protein<sup>21–23</sup> and  $\alpha$ -hemolysin,<sup>24</sup> by making target protein–PYP hybrids. As just described, this strategy places rather strict constraints on the target proteins that can be controlled because linkage sequences that satisfy functional constraints of both PYP and the target protein must be chosen.<sup>1,21–23</sup>

We reasoned that construction of a circularly permuted PYP variant might lead to a relaxation of these sequence constraints. Ramachandran et al. have reported that distances between residues near the N-terminus of PYP (Ala5 and Glu9) and a residue on a loop adjacent to the C-terminus (Gln99) change

**Received:** January 7, 2013

**Revised:** April 8, 2013

**Published:** April 10, 2013



by up to 19 Å upon PYP isomerization to the light state.<sup>a,20</sup> We hypothesized that if the N- and C-termini of PYP were linked in a circular permutant, the conformation, dynamics, and end-to-end distance of the linker would be changed significantly if the main aspects of the light-triggered protein structural change were preserved. A variety of target sequences with bioactivity, but few restraints on sequence, could then be introduced as linkers and may be subject to photocontrol.

Our aim in this work was to test if circular permutation can be accomplished using an unstructured flexible linker while preserving the light-driven conformational changes of PYP.

## MATERIALS AND METHODS

**Gene Synthesis and Site-Directed Mutagenesis.** DNA encoding cPYP (codon optimized for *Escherichia coli*) was synthesized by BioBasic Inc. (Toronto, ON) and inserted into the pET24b(+) vector using NdeI and HindIII restriction sites. The gene for wild-type PYP was cloned into the same vector.<sup>21</sup> Mutations to create M100E-PYP, M121E-cPYP, and M121A-cPYP were introduced using standard molecular biology protocols. Primers for the mutations were designed with PrimerX (<http://www.bioinformatics.org/primerx/>) following the Stratagene QuikChange protocol (Agilent, Inc.) and purchased from ACGT Corp. Primers for the M100E mutation: forward, 5' CACCTTCGATTACCAAGAGACGCCACGAAGGTG 3'; and reverse, 5' CACCTTCGTGGGCGTCTCTTGGAATCGAAGGTG 3'. Primers for the M121E mutation: forward, 5' GAATACACCTTCGACTACCAGGAGACGCCAACTAAAGTAAAAG 3'; reverse, 5' CTTTACTTTAGTTGGCGTCTCTGGTAGTCGAAGGTGTATTTC 3'. Primers for the M121A mutation: forward, 5' GAATACACCTTCGACTACCAGGCGACGCCAACTAAAGTAAAAG 3'; reverse, 5' CTTTACTTTAGTTGGCGTCTCGCTGGTAGTCGAAGGTGTATTTC 3'.

For each mutation, 100 ng each of the forward and reverse primers were added to 50 ng of template DNA, 25 µL of *Pfu Turbo* hotstart polymerase chain reaction (PCR) master mix [a 2× formulation of *Pfu Turbo* hotstart DNA polymerase, an optimized PCR reaction buffer, magnesium, and dNTPs (Agilent Technologies)], and water in a total volume of 50 µL. The reaction mixture was held at (i) 95 °C for 2 min followed by (ii) 30 s at 95 °C, (iii) 30 s at 5 °C below primer  $T_m$ , and (iv) 6 min at 72 °C. Steps ii–iv were repeated 30 times, and then the mixture was held at 72 °C for an additional 10 min before being allowed to cool to room temperature. A 1 µL aliquot of DpnI was added to the reaction mixture, which was then incubated at 37 °C for 1 h. A 0.8% agarose gel in 0.5× TBE was run to check for PCR products. A PCR purification kit (Invitrogen) was subsequently used, and the product was transformed into MAX Efficiency DH5α competent cells (Invitrogen). A midprep (Invitrogen) was conducted, and the plasmids were sequenced in both directions (ACGT Corp.) to confirm the mutations.

**Protein Expression and Purification.** Expression and reconstitution of the PYP constructs were adapted from the work of Devanathan et al.<sup>25</sup> The protocol was the same for all constructs. DNA (0.2 ng) was transformed into BL21\*(DE3) competent cells and plated onto agar plates containing 30 µg/mL kanamycin. The following day, a single colony was used to inoculate 25 mL of Luria-Bertani (LB) broth that had been supplemented with kanamycin (30 µg/mL). The 25 mL overnight culture was used to inoculate 1 L of LB supplemented with 30 µg/mL kanamycin. Cells were grown

at 37 °C until an OD<sub>600</sub> of 0.6 was reached and then induced with 1 mM IPTG. The temperature was adjusted to 25 °C, and the cells were grown for a further 1.5 h before 25 mg of activated chromophore dissolved in 1 mL of ethanol was added to the medium. The synthesis of the activated chromophore, 4-hydroxycinnamic acid S-thiophenyl ester, was conducted as detailed by Changuet-Barret et al.,<sup>26</sup> except that the product was not recrystallized. The cells were grown for a further 6 h before being centrifuged to separate the medium from the protein-containing cell pellet.

The pellet was resuspended in lysis buffer containing 50 mM sodium phosphate (pH 8.0), 300 mM sodium chloride, and 5 mM magnesium chloride and frozen at –20 °C until it was purified. The resuspended cell pellet was sonicated in pulses on ice for 5 min and then centrifuged at 12K rpm for 1 h to separate the supernatant from the pellet. The protein was purified on a Ni-NTA column that was equilibrated with lysis buffer. The protein-containing supernatant was loaded onto the column, and the yellow color became associated with the resin. The resin was washed with 10 column volumes (CV) of the lysis buffer. The resin was subsequently washed with 5 CV of high-salt buffer (i.e., lysis buffer supplemented with 2 M NaCl) followed by a further 5 CV of lysis buffer. To elute nonspecifically bound proteins, the resin was subjected to 5 CV of lysis buffer supplemented with 5 mM imidazole. The protein was eluted by increasing the concentration of imidazole to 200 mM.

The eluted protein was dialyzed extensively against 40 mM Tris-OAc, 1 mM EDTA, and 100 mM NaCl (pH 7.5) [1× TAE and 100 mM NaCl (pH 7.5)] at 4 °C. The dialyzed protein was concentrated to ~1.5 mL using an Amicon ultracentrifugal device [10000 Da NMWL (nominal molecular weight limit) (Millipore)]. The protein was then applied to a Superdex 75 10/300 GL column (GE Healthcare) running in 1× TAE, 100 mM NaCl buffer (pH 7.5). UV–vis absorbance spectroscopy was used to determine which eluted fractions had the highest ratios of absorbance at 446 nm to that at 278 nm. A value of ~2 was typical for pure wtPYP or cPYP holoprotein and 1.4 for M100E-PYP and M121E-CPYP. The purity and identity of samples were confirmed using 12.5% sodium dodecyl sulfate–polyacrylamide gel electrophoresis and electrospray ionization mass spectrometry (ESI-MS). The expression levels of all three constructs were similar; a 1 L culture routinely gave >25 mg of purified protein.

**UV–Vis Spectra and Photoisomerization.** UV–vis spectral and kinetic measurements were performed using a PE Lambda 35 or 25 spectrophotometer or using a diode array UV–vis spectrophotometer (Ocean Optics Inc., USB4000) in each case, coupled to a temperature-controlled cuvette holder (Quantum Northwest, Inc.). Protein concentrations were determined using an extinction coefficient at  $\lambda_{max}$  (~446 nm) of  $45 \times 10^3 \text{ M}^{-1} \text{ cm}^{-1}$  for wtPYP and cPYP and  $29 \times 10^3 \text{ M}^{-1} \text{ cm}^{-1}$  for M100E-PYP and M121E-CPYP. Irradiation of the protein sample was conducted using a Luxeon III Star LED Royal Blue (455 nm) Lambertian instrument operating at approximately 700 mA (~50 mW/cm<sup>2</sup>). To determine the rate constants for thermal relaxation, changes in the absorbance spectrum at 350 nm were monitored. Data were fit to single-exponential functions to extract rate constants.

**pH Effects.** Studies of pH effects were conducted in a universal buffer (25 mM sodium acetate, MES, Tris, and CAPSO and 100 mM NaCl) in a 1.0 cm path length quartz cuvette using a PE Lambda 25 spectrophotometer. To obtain

different pH values, the samples were titrated with 1 M HCl or 1 M NaOH and then stirred for 1 min. The rate constants for thermal relaxation were obtained by irradiating the sample for 1 min using a Luxeon III Star LED Royal Blue (455 nm) Lambertian instrument operating at approximately 700 mA ( $\sim 50$  mW/cm<sup>2</sup>), and changes in the absorbance at 350 nm were monitored at 20 °C. Data were analyzed as described above.

**Thermal Stability.** Samples were prepared in 1× TAE and 100 mM NaCl (pH 7.5). Samples were fully dark adapted before they were scanned in the UV–vis region from 250 to 550 nm. At each temperature, the samples were allowed to equilibrate for 5 min before spectra were collected. The contribution from the buffer was subtracted from the protein spectra.

**Salt Effects.** All studies were performed in 1× TAE buffer and 100 mM NaCl (pH 7.5) having 0.5, 1, or 2 M (NH<sub>4</sub>)<sub>2</sub>SO<sub>4</sub> or NH<sub>4</sub>Cl at 20 °C. Samples were fully dark adapted before they were scanned in the UV–vis region from 250 to 550 nm.

**Guanidinium Denaturation Studies.** Guanidinium-induced denaturation of wtPYP, cPYP, and M121E-cPYP was monitored by tryptophan (Trp) fluorescence using an Aviv Associates (Lakewood, NJ) model ATF 105 automated titrating spectrofluorometer. Protein samples ( $\sim 5$  μM) were prepared in 1× TAE and 100 mM NaCl (pH 7.5) with or without 5 M GdnHCl (ThermoFisher) and allowed to incubate overnight to fully dark adapt. Both folding and unfolding titrations were performed. The fluorescence of protein samples was acquired using excitation at 280 nm and emission at 360 nm with a bandwidth of 2 nm. During the fluorescence experiment, the sample volume was kept constant at 2 mL, with a 1.0 cm path length quartz cuvette, and the temperature was maintained at 20 °C. The sample was stirred after each addition for 1 min, and then stirring was halted before the fluorescence measurement. Fluorescence data were fit using the equation

$$F_{360} = (\alpha_N + \beta_N[\text{Gdn}] + \{\alpha_D + \beta_D[\text{Gdn}]\} \exp[m_{D-N}([\text{Gdn}] - [\text{D}]^{50\%})/RT]) / \{1 + \exp[m_{D-N}([\text{Gdn}] - [\text{D}]^{50\%})/RT]\}$$

where  $\alpha_N$  is  $F_{360}$  in the absence of guanidinium,  $\beta_N$  is the slope ( $F_{360}$  vs  $[\text{Gdn}]$ ) at the beginning of the curve,  $\alpha_D$  is the value of  $F_{360}$  for the fully denatured state, and  $\beta_D$  is the slope at the end of the transition. The quantity  $[\text{D}]^{50\%}$  is the Gdn concentration at the point where the protein is 50% unfolded, and the term  $m_{D-N}$  is a constant that reflects the degree of unfolding of the protein in guanidinium.<sup>27</sup>

**CD Measurements.** CD experiments were conducted on an Olis RSM100 CD instrument. Samples were prepared at a final concentration of 15 μM in 1 mM sodium phosphate buffer (pH 7.5). A cylindrical quartz cell with a 0.1 cm path length was used for all measurements. Samples were fully dark adapted before they were scanned in the far-UV region from 260 to 190 nm at 20 °C. The integration time was 2 s, and three scans were averaged to give a final spectrum. For the irradiated state, samples were irradiated using a Luxeon III Star LED Royal Blue (455 nm) Lambertian instrument operating at approximately 700 mA (50 mW/cm<sup>2</sup>) for 1 min, and five individual sets were averaged to obtain the final spectrum. Buffers were also scanned under the same conditions and subtracted from the protein spectra. The spectra were converted to mean residue

ellipticities and smoothed using a binomial algorithm in IgorPro (Wavemetrics).

**Sedimentation Equilibrium.** Samples of M121E-cPYP were prepared at concentrations of 5.5, 11.1, and 22.2 μM in 1× TAE, 100 mM NaCl buffer (pH 7.5) and analyzed by analytical ultracentrifugation (AUC facility, Department of Biochemistry, University of Toronto). Absorbance at 446 nm was monitored at 4 °C and speeds of 20000 and 24000 rpm.

**NMR.** Labeled protein samples (<sup>15</sup>N-labeled, <sup>15</sup>N- and <sup>13</sup>C-labeled, and <sup>19</sup>F-labeled cPYP, M121E-cPYP, and M100-PYP) were prepared as follows. An expression plasmid was transformed into BL21\*(DE3) chemically competent cells, and these were plated on LB agar plates supplemented with 30 μg/mL kanamycin. The following day, a single colony from the agar plate was used to inoculate 25 mL of LB broth/kanamycin medium, and the culture was incubated overnight at 37 °C and 250 rpm. The following day, 6 mL of the overnight culture was centrifuged for 15 min at 4000 rpm, and the pellet was resuspended in 50 mL of M9 medium containing a natural abundance of <sup>15</sup>N. The 50 mL culture was grown at 37 °C and 250 rpm until it had reached midlog phase ( $\text{OD}_{600} \sim 0.5\text{--}0.7$ ), and then it was centrifuged as described above. The pellet was used to inoculate 1 L of 99% <sup>15</sup>N-enriched M9 minimal medium, supplemented with 0.3% D-glucose, 0.1% <sup>15</sup>NH<sub>4</sub>Cl (Cambridge Isotope Laboratories, Inc.), 30 mg/L kanamycin, 10 mg/L thiamine, 10 mg/L biotin, 1 mM MgSO<sub>4</sub>, 1 mM CaCl<sub>2</sub>, and 1% Bioexpress cell growth <sup>15</sup>N medium (Cambridge Isotope Laboratories, Inc.), and the culture was subsequently grown at 37 °C and 250 rpm until it had again reached midlog phase. At an  $\text{OD}_{600}$  of 0.6, protein expression was induced by the addition of 1 mM IPTG. The temperature was adjusted to 25 °C, and the cells were grown for a further 1.5 h, after which 25 mg of activated chromophore<sup>26</sup> dissolved in 1 mL of ethanol was added. The temperature was then adjusted to 18 °C, and the culture was grown overnight. The following day, the cells were harvested by centrifugation at 4000 rpm and 4 °C for 1 h. For doubly (<sup>15</sup>N and <sup>13</sup>C) labeled protein samples, <sup>13</sup>C-enriched D-glucose (Cambridge Isotope Laboratories, Inc.) replaced unlabeled glucose in the medium, and 1% Bioexpress cell growth medium enriched with both <sup>15</sup>N and <sup>13</sup>C was added in place of medium that was enriched with only <sup>15</sup>N. To introduce fluorotryptophan into M100E-PYP and M121E-cPYP, <sup>19</sup>F-labeled 5-fluoro-L-D-Trp (Aldrich) was added to the bacterial culture at a concentration of 60 mg/L, 1 h prior to induction.<sup>28</sup> Here, activated chromophore addition was conducted together with induction of protein expression by addition of 1 mM IPTG, and growth was halted 2 h after induction. The protein was purified in the same manner as unlabeled samples (as described above). The mass of the protein was confirmed by electrospray ionization mass spectrometry.

Samples were placed in a Shigemi tube (BMS-005TV, Shigemi, Inc.) with a multimode 1 mm fiber optic (Thorlabs) inserted through the top. The other end of the fiber was coupled to a Royal Blue LED [LXH-LR5C (700 mW), LED Supply] through a focusing lens (WPI, Inc.). Tests outside the NMR magnet confirmed that this irradiation setup would completely convert M100E-PYP and M121E-cPYP into their colorless light states.

NMR experiments were conducted at the Québec/Eastern Canada High Field NMR Facility or at CSICOMP (Department of Chemistry, University of Toronto). Experiments for backbone assignments were performed using a 500 MHz Varian



Inova spectrometer equipped with a z-gradient HCN 5 mm cold probe. All pulse sequences were used as obtained from the Varian “Biopack” sequence library. HSQC spectra were acquired with 40 increments spanning 1520 Hz in the  $^{15}\text{N}$  dimension. Backbone assignments were determined from HNCO<sup>29</sup> (32  $^{13}\text{C}$  increments spanning 1510 Hz), HNCACB<sup>30</sup> (64  $^{13}\text{C}$  increments spanning 8300 Hz), CBCA(CO)NH<sup>31</sup> (48  $^{13}\text{C}$  increments spanning 8300 Hz), and C(CO)NH<sup>32</sup> (80  $^{13}\text{C}$  increments spanning 9040 Hz) spectra, all acquired with 32 increments spanning 1520 Hz in the  $^{15}\text{N}$  dimension. For the C(CO)NH spectra, mixing of  $^{13}\text{C}$  magnetization was achieved using a FLOPSY8<sup>33</sup> mixing scheme applied for 12.7 ms.

Spectra were processed using the NMRPipe<sup>34</sup> processing suite. Typically, FID signals were zero-filled to double the original data size and apodized using a squared-cosine window function prior to Fourier transformation. In the indirect dimension(s), linear prediction was used to double the original data size prior to zero-filling and apodization as described above. Assignment of backbone resonances was performed using standard methods,<sup>35</sup> aided by NMRViewJ (One Moon Scientific).

$^{19}\text{F}$  one-dimensional NMR experiments were performed at different temperatures on a 700 MHz Agilent DD2 spectrometer, using a H-F{ $^{13}\text{C}$ ,  $^{15}\text{N}$ } triple-resonance cold probe, in which the high-frequency channel could be tuned to  $^{19}\text{F}$ . At least 1024–16384 scans were used to obtain the  $^{19}\text{F}$  NMR spectrum in dark and irradiated states (typically, spectra acquired at lower temperatures required more scans). A 300  $\mu\text{L}$  sample volume was used in a 3 mm sample tube, with a fiber optic inserted, inserted into a 5 mm sample tube containing a reference solution of trifluoroacetic acid (TFA). Spectra were referenced to the chemical shift of TFA (−78.5 ppm) and processed using 50 Hz line broadening. Lorentzian fitting was used to obtain chemical shifts. Photoswitching was accomplished in the same manner as described above.

## RESULTS AND DISCUSSION

**Protein Design.** To test if a circularly permuted PYP would fold normally and undergo a native photocycle, we decided to introduce a simple flexible linker (GGSGGSGG) long enough to link the N- and C-termini but chosen to be minimally perturbing to the PYP scaffold. We opted to create new N- and C-termini at G115 and S114, because this is the loop most distant from the chromophore and mutations here, unlike other loops, have not been found to cause significant changes in the properties of PYP.<sup>15</sup> A model of this circularly permuted PYP (cPYP) protein is shown in Figure 1.

**Structural Characterization of Dark-Adapted cPYP.** The circularly permuted PYP expressed well and was highly soluble. UV–vis spectra of the dark-adapted states of wtPYP and cPYP at pH 7.5 are shown in panels c and d of Figure 1, respectively. The spectra are virtually superimposable, and this was found to be the case at pH 5.0 and 9.0 as well (not shown). Constant-intensity ( $\sim 50\text{ mW/cm}^2$ ) 450 nm irradiation gave the steady-state (irradiated) spectra shown as dotted lines in panels c and d of Figure 1. Whereas the magnitude of the peak at 446 nm is greatly decreased and a peak appears at 350 nm for wtPYP, as expected for significant conversion to the cis, protonated form of the protein, the changes are much less pronounced for the cPYP species. As detailed below, this observation is a consequence of the significantly faster thermal relaxation rate of the cPYP cis species to the dark-adapted, trans

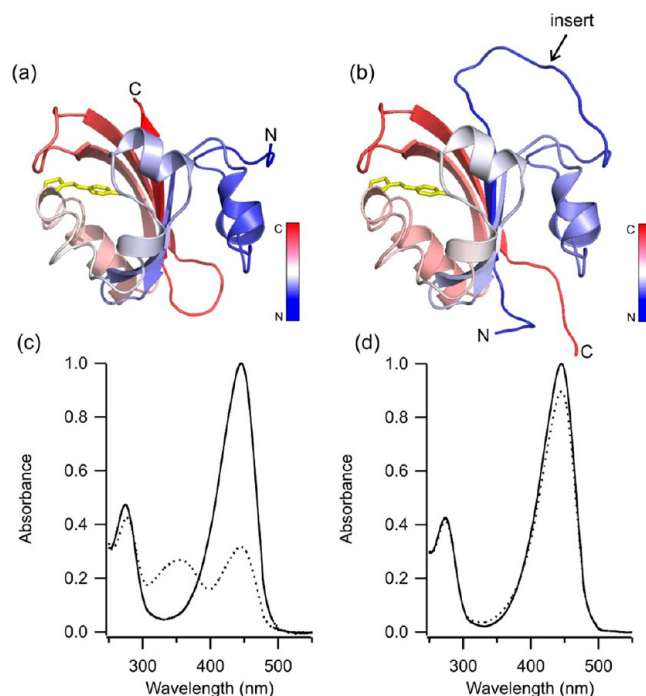


**Figure 1.** Models of (a) wtPYP and (b) cPYP in the dark-adapted state colored in a gradient from the N-terminus (blue) to the C-terminus (red) on the basis of the high-resolution X-ray structure of dark-adapted PYP [Protein Data Bank (PDB) entry 1NWZ].<sup>36</sup> The chromophore is shown as yellow sticks. The GGSGGSGG insert is modeled as a flexible loop. (c) UV–vis spectrum of wtPYP: dark-adapted (—) or irradiated with 450 nm light (···) (pH 7.5, Tris-acetate EDTA buffer, 100 mM NaCl, 20 °C). (d) UV–vis spectrum of cPYP: dark-adapted (—) or irradiated with 450 nm light (···) (pH 7.5, Tris-acetate EDTA buffer, 100 mM NaCl, 20 °C).

isomer. We focus first on the structure of the dark-state cPYP protein and on the extent to which this resembles wtPYP.

CD spectra of wtPYP and cPYP at pH 7.5 are shown in Figure 2a. These are very similar, indicating the overall secondary structures of the two proteins are very similar. A temperature denaturation experiment indicated cPYP was nearly as stable as the wild type (Figure 2b). Reversible denaturation with guanidinium was also measured (Figure 2c), and cPYP was found to undergo a cooperative folding–unfolding transition, although it was distinctly less stable than wtPYP as judged by the concentration of guanidinium at the midpoint of the denaturation curve. This result is typical for circularly permuted proteins.<sup>37</sup>

To obtain a more detailed assessment of the similarity of the dark-state structure of cPYP to that of wtPYP, we expressed  $^{15}\text{N}$ - and  $^{13}\text{C}$ -labeled protein and assigned the backbone chemical shifts using standard protein NMR methods (see the Supporting Information). The  $^{15}\text{N}$ – $^1\text{H}$  HSQC spectra of wtPYP and cPYP are shown overlaid in Figure 3 together with a model of the cPYP structure based on the X-ray structure of wtPYP (as in Figure 1b), with residues colored according to their level of chemical shift similarity to wtPYP. There is very close correspondence of chemical shifts across the chromophore binding domain. There are large changes in chemical shifts at the loop where the new N- and C-termini were created as expected. There are smaller changes in parts of the N-terminal cap domain, including the Trp indole NH signal. The glycine rich linker connecting the wild-type N- and C-termini

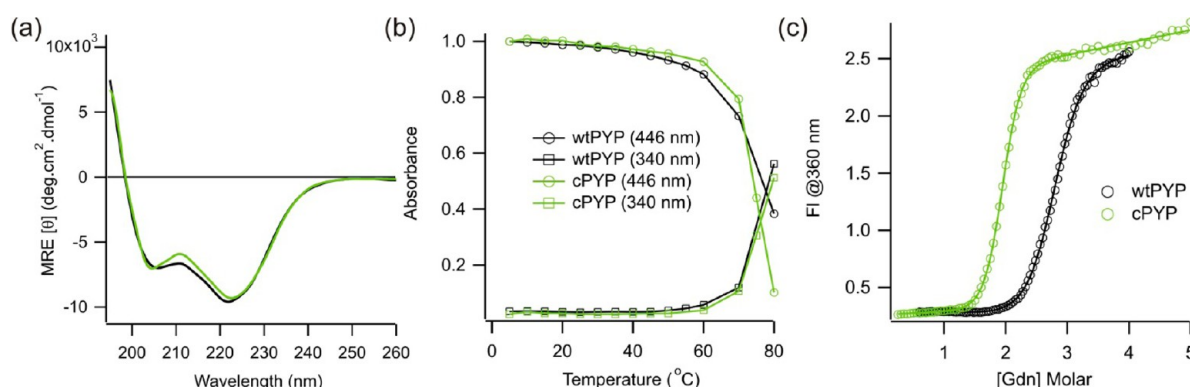


**Figure 2.** (a) Circular dichroism spectra of dark-adapted wtPYP (black) and cPYP (green) (pH 7.5, 5 mM sodium phosphate buffer, 20 °C). (b) Temperature denaturation titrations of dark-adapted wtPYP (black) and cPYP (green) (pH 7.5, Tris-acetate EDTA buffer, 100 mM NaCl). (c) Guanidinium refolding curve for dark-adapted wtPYP (black) and cPYP (green) (pH 7.5, Tris-acetate EDTA buffer, 100 mM NaCl, 20 °C).

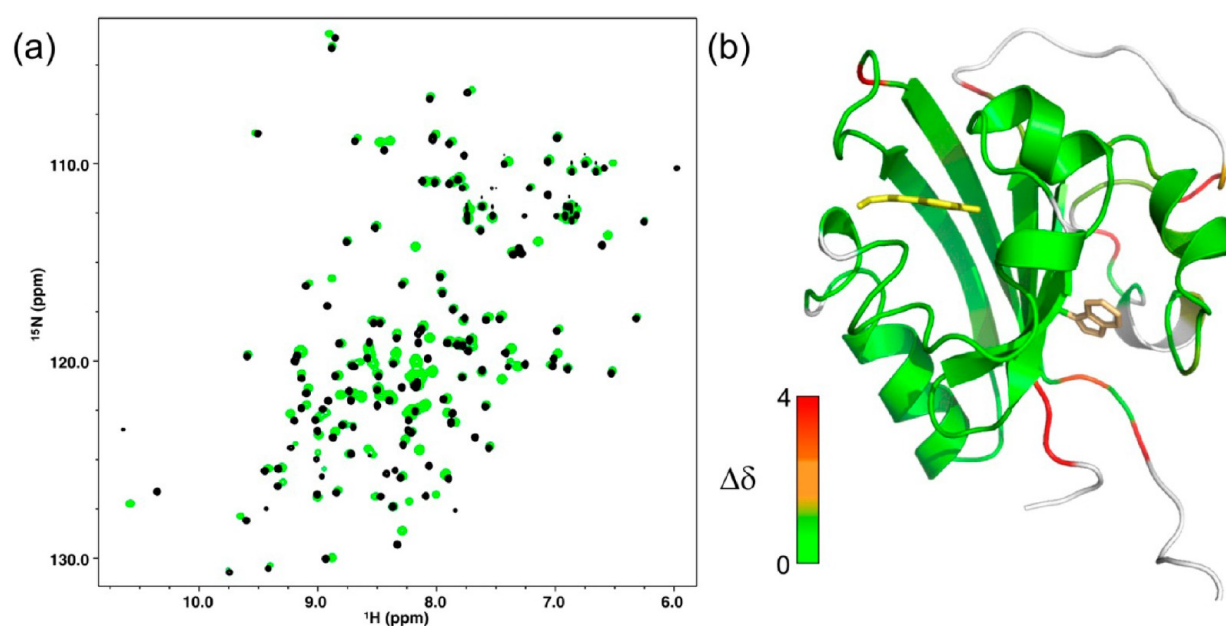


**Figure 3.** (a)  $^{15}\text{N}$ - $^1\text{H}$  HSQC spectrum of wtPYP (black) and cPYP (green). For assignments, see the Supporting Information. (b) Modeled structure of cPYP (based on wt PYP, PDB entry 1NWZ)<sup>36</sup> with residues colored according to chemical shift difference from wtPYP (BMRB entry 18122).<sup>38</sup> The chemical shift difference was calculated as  $\Delta\delta = [(\Delta\delta^{15}\text{N})^2]^{1/2} + 5[(\Delta\delta^1\text{H})^2]^{1/2}$ . The Trp side chain is shown as orange sticks. Note that the indole NH peak moves relative to wtPYP (pH 7.5, Tris-acetate EDTA buffer, 100 mM NaCl, 20 °C). This model was produced using PyMol.

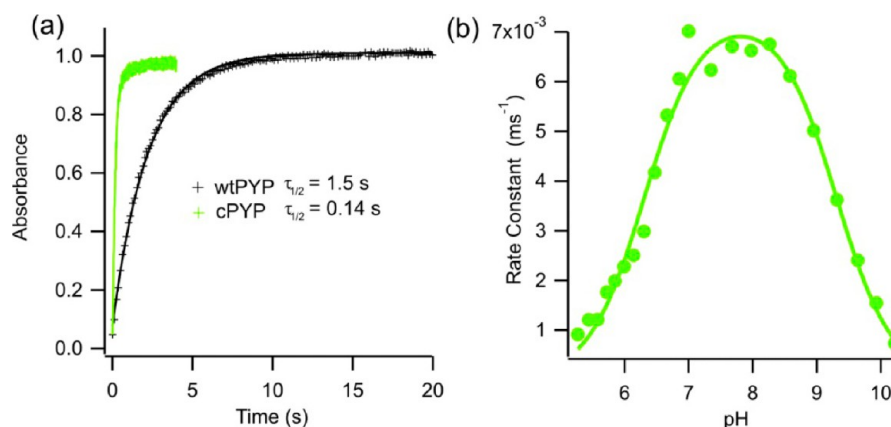


**Figure 4.** (a) Recovery of dark-adapted wtPYP (black) and cPYP (green) after irradiation with 450 nm light (pH 7.5, Tris-acetate EDTA buffer, 100 mM NaCl, 20 °C). (b) pH dependence of dark-state recovery of cPYP as a function of pH (100 mM NaCl, 20 °C). The fitted curve is given by the equation  $k_{\text{obs}} = k_{\text{max}} / (1 + 10^{\text{pK}_1 - \text{pH}} + 10^{\text{pH} - \text{pK}_2})$  with a  $\text{pK}_1$  of  $6.3 \pm 0.1$  and a  $\text{pK}_2$  of  $9.3 \pm 0.1$ .

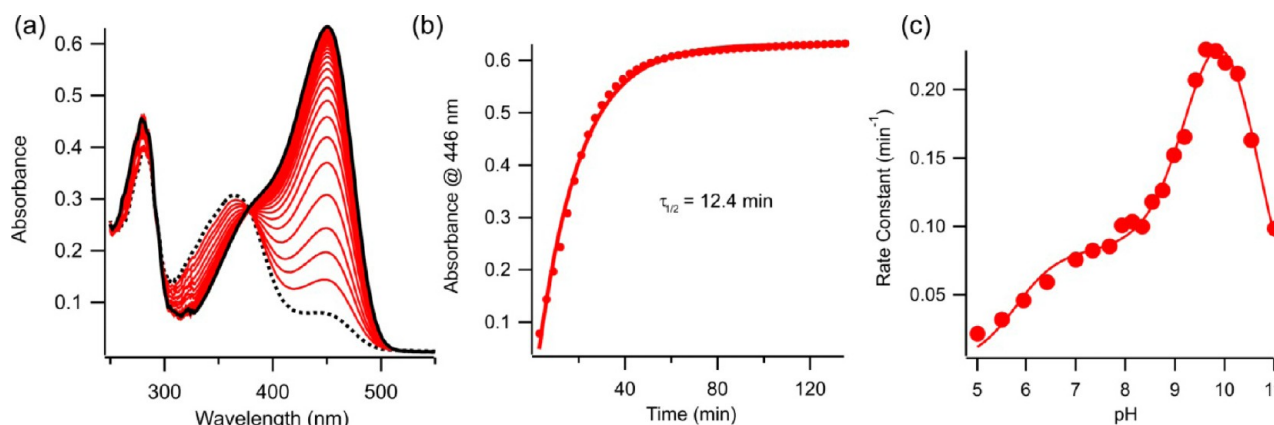


**Figure 5.** (a) UV-vis spectrum of M121E-cPYP [dark-adapted (—) and irradiated with 450 nm light (···) (pH 7.5, Tris-acetate EDTA buffer, 100 mM NaCl, 20 °C)]. (b) Recovery of dark-adapted M121E-cPYP after irradiation with 450 nm light (pH 7.5, Tris-acetate EDTA buffer, 100 mM NaCl, 20 °C). (c) pH dependence of the dark-state recovery rate of M121E-cPYP as a function of pH (100 mM NaCl, 20 °C). The fitted curve is given by the equation  $k_{\text{obs}} = k_{\text{max1}} / (1 + 10^{pK_1 - \text{pH}} + 10^{\text{pH} - pK_2}) + k_{\text{max2}} / (1 + 10^{pK_2 - \text{pH}} + 10^{\text{pH} - pK_3})$  with a  $pK_1$  of  $5.8 \pm 0.1$ , a  $pK_2$  of  $9.3 \pm 0.1$ , and a  $pK_3$  of  $10.6 \pm 0.1$ .

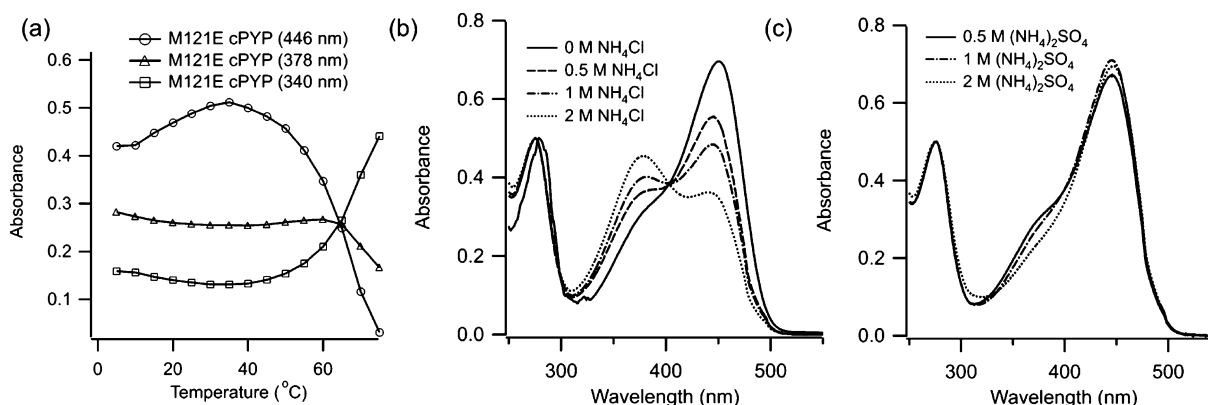


**Figure 6.** (a) Measured absorbance of dark-adapted M121E-cPYP (dark-adapted in pH 7.5, Tris-acetate EDTA buffer, 100 mM NaCl) at a series of temperatures. (b) UV-vis spectrum of dark-adapted M121E-cPYP (pH 7.5, Tris-acetate EDTA buffer, 100 mM NaCl) with the addition of the indicated concentration of ammonium chloride. (c) UV-vis spectrum of dark-adapted M121E-cPYP (pH 7.5, Tris-acetate EDTA buffer, 100 mM NaCl) with the addition of the indicated concentration of ammonium sulfate.

could not be assigned presumably because of the overlap of resonances and/or mobility of the segment. Overall, these data indicate that the dark-adapted structures of cPYP and wtPYP are very similar, although local changes to structure and/or dynamics in the N-terminal cap are likely.

**Rapid Photoswitching of cPYP.** We next investigated the photoswitching characteristics of cPYP. Figure 4 shows the recovery of the dark-state structure as monitored by UV-vis spectroscopy after removal of blue light irradiation. The rate constant for the cis-to-trans recovery of cPYP is seen to be  $\sim 10$  times faster than that of wtPYP at pH 7.5 and 20 °C. This enhanced recovery rate is also seen at lower and higher temperatures (not shown). The enhanced recovery rate explains the smaller change in steady-state spectra observed under constant low-intensity blue light irradiation (Figure 1c,d). We measured the relaxation rate of cPYP as a function of pH (Figure 4b) and found a bell-shaped dependence of the relaxation rate with a maximum near pH 7.8 and apparent  $pK_a$  values of 6.3 and 9.3. This pH dependence is very similar to that of wild-type PYP for which apparent  $pK_a$  values of 6.4 and 9.4 were reported.<sup>39</sup>

The rapid thermal recovery of the dark-state structure of cPYP is rather unusual; to the best of our knowledge, although

PYP homologues from other species that undergo rapid thermal recovery have been identified, all mutations or modifications of wtPYP from *Halorhodospira halophila* reported to date have resulted in varying degrees of deceleration of the recovery rate.<sup>15,18</sup> From the point of view of using cPYP as a photoswitch to control biomolecular function, the very rapid thermal recovery is problematic because it means that only a small fraction of the cis state can be populated under steady-state conditions with common light sources (Figure 1d). We therefore wished to modify cPYP to slow its thermal recovery rate.

A number of modifications to wtPYP result in a dramatic slowing of the thermal recovery rate.<sup>15</sup> The best characterized of these are deletions to the N-terminal domain (1–25) and point mutations at M100. Because we wished to maintain the conformational changes at the N-terminus, we chose to mutate M100 (M121 in cPYP sequence numbering).

**M121E-cPYP Exhibits a Slower Photocycle.** The M121A and M121E point mutations of cPYP were created, expressed, and purified. The two proteins behaved very similarly so that only one (M121E-cPYP) was studied in detail. Figure 5 shows UV-vis spectra of this species under dark-adapted conditions together with steady-state spectra observed under 450 nm



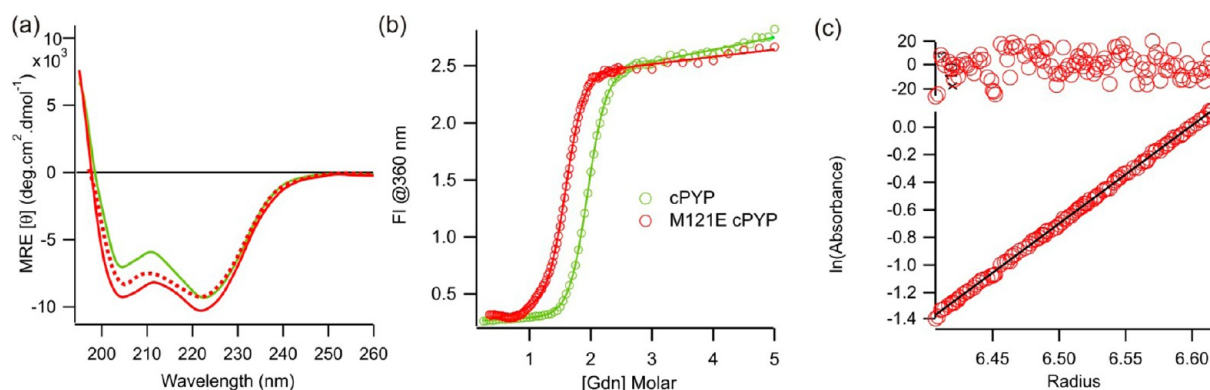


**Figure 7.** (a) Circular dichroism spectra of dark-adapted M121E-cPYP (red), irradiated (450 nm) M121E-cPYP (red dotted), and cPYP (green) (pH 7.5, 5 mM sodium phosphate buffer, 20 °C). (b) Guanidinium refolding curve of dark-adapted M121E-cPYP (red) and cPYP (green) (pH 7.5, Tris-acetate EDTA buffer, 100 mM NaCl, 20 °C). (c) Sedimentation equilibrium data (linear fit and residuals) indicating that M121E-cPYP (pH 7.5, Tris-acetate EDTA buffer, 100 mM NaCl) behaves as a monomer.

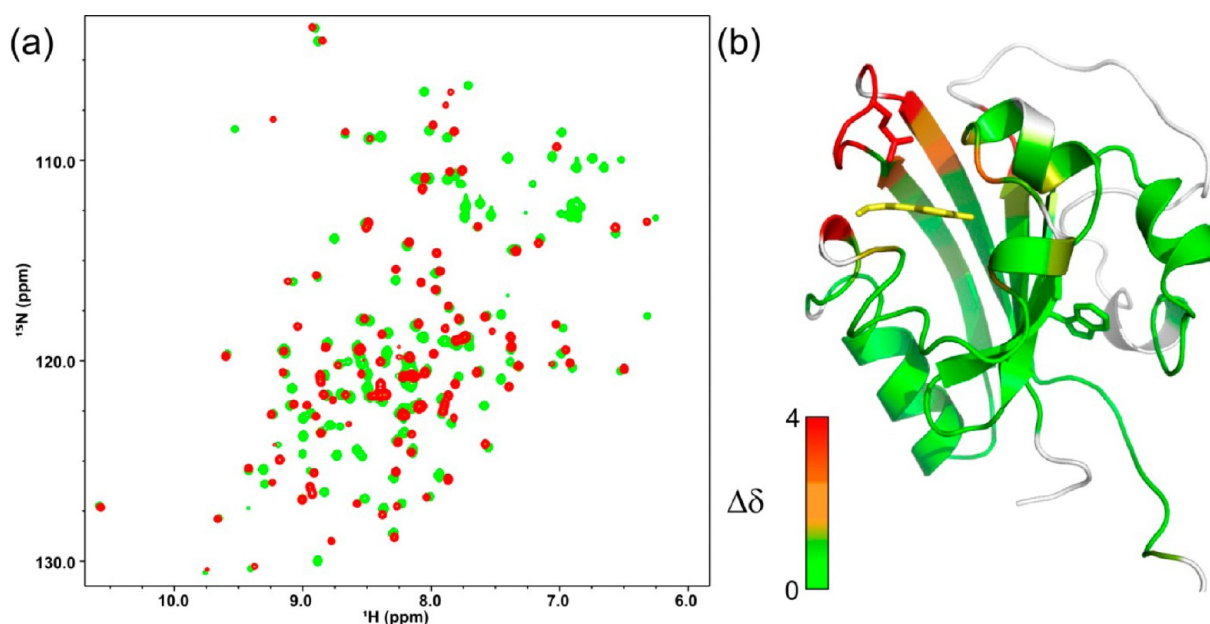


**Figure 8.** (a)  $^{15}\text{N}$ – $^1\text{H}$  HSQC spectrum of cPYP (green) and M121E-cPYP (red). For assignments, see the Supporting Information. (b) Modeled structure of M121E-cPYP (based on wtPYP, PDB entry 1NWZ) with residues colored according to chemical shift difference from cPYP. The chemical shift difference was calculated as  $\Delta\delta = [(\Delta\delta^{15}\text{N})^2]^{1/2} + 5[(\Delta\delta^1\text{H})^2]^{1/2}$ . The Trp side chain is shown as green sticks; the indole NH group has identical chemical shifts in cPYP and M121E-cPYP. This model was produced using PyMol.

irradiation. Thermal recovery of the dark state was found to occur with a half-life of 12.4 min at pH 7.5, ~500 times longer than with cPYP (Figure 5b). The pH dependence of the reisomerization rate was found to be more complex than for cPYP with a maximum near pH 10 and three apparent  $pK_a$  values. Throughout the entire pH range, however, the recovery rate was slow enough that complete isomerization to the cis form could be easily achieved under steady-state blue light illumination.

An examination of the dark-state UV–vis spectrum of M121E-cPYP (Figure 5a) compared to that of cPYP (Figure 1d) reveals the presence of a shoulder at ~380 nm in addition to the main absorbance band at 446 nm expected for the deprotonated trans form of the chromophore. The 380 band, called an “intermediate spectral form”,<sup>40</sup> has been observed previously in M100E, M100A, and M100L mutants of wtPYP as well as in the Y42F wtPYP mutant. The band has been ascribed to the presence of a fraction of protonated trans

chromophore in the dark-adapted protein.<sup>40–42</sup> In wtPYP (and by extension cPYP), the pCA phenolic proton is completely transferred to Glu46 so that only the anionic form of the chromophore is observed. A mutation such as M100E (M121E in cPYP) or Y42F appears to alter the balance of  $pK_a$  values so that two distinct H-bonding arrangements coexist, one of which involves the protonated chromophore. Because the H-bonding equilibrium involves two sites on the protein, not an equilibrium between the solvent and protein, changing the bulk pH does not substantially affect the UV–vis spectrum (see the Supporting Information). The ratio of protonated to anionic chromophore is affected by temperature, however. Figure 6 shows that the fraction of the anionic chromophore is maximal at 35 °C and decreases below this temperature. Above 35 °C, the fraction of the anionic chromophore also decreases, and ultimately, the protein unfolds near 60 °C. Chaotropic salts such as ammonium chloride stabilize the protonated form of

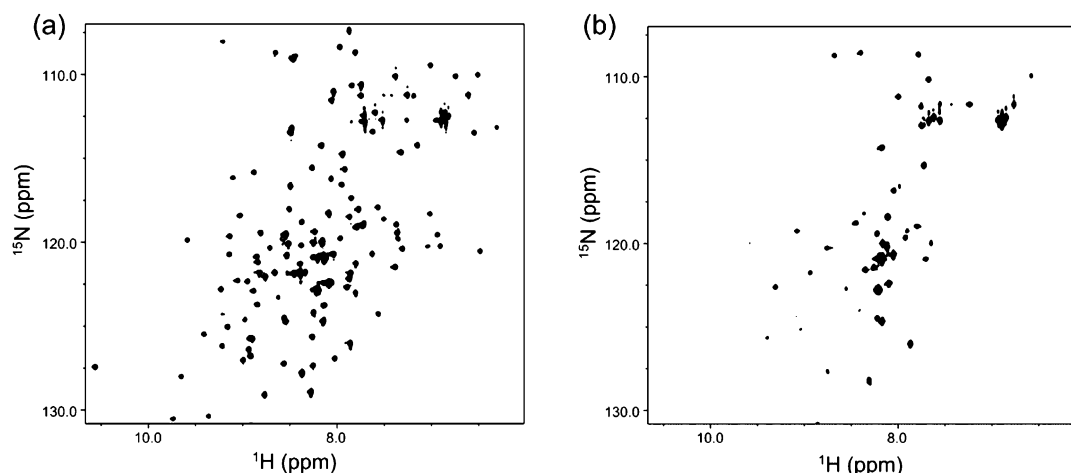


**Figure 9.**  $^{15}\text{N}$ – $^1\text{H}$  HSQC spectrum of M121E-cPYP in dark-adapted (a) and irradiated (b) states.

the chromophore, whereas kosmotropic salts stabilize the anionic form (Figure 6b,c).

**Structural Characterization of Dark-Adapted M121E-cPYP.** We wished to test whether the dark-state structure and the light-driven conformational changes were preserved in M121E-cPYP compared to cPYP and wtPYP. We first compared the CD spectrum of M121E-cPYP to those of cPYP and wtPYP (Figure 7a). These spectra were normalized using the absorbance of the protonated pCA chromophore at 350 nm after denaturation of the proteins in 2% SDS. The CD spectrum of M121E-cPYP exhibits slightly more negative ellipticity near 208 nm relative to cPYP and wtPYP. It is unclear if this represents a slightly larger fraction of helical secondary structure versus that of cPYP or whether the optical changes associated with the presence of a fraction of the protonated chromophore produce alterations in this region of the CD spectrum.

Reversible denaturation by guanidinium was also measured (Figure 7b), and M121E-cPYP was found to undergo a cooperative folding–unfolding transition. The M121E-cPYP mutant was somewhat less stable than cPYP as judged by the concentration of guanidinium at the midpoint of the denaturation curve.

Because circularly permuted proteins can sometimes form domain-swapped dimers,<sup>43,44</sup> we checked for self-association of M121E-cPYP by analytical ultracentrifugation (Figure 7c). These data indicated that the protein behaves as a monomer under the solution conditions tested.

To obtain a more detailed assessment of the similarity of the dark-state structure of M121E-cPYP to cPYP and wtPYP, we again compared backbone chemical shifts obtained using standard protein NMR methods (see the Supporting Information). The  $^{15}\text{N}$ – $^1\text{H}$  HSQC spectra of M121E-cPYP and cPYP are shown overlaid in Figure 8 together with a model colored according to chemical shift similarity. There is very close correspondence of chemical shifts throughout the central  $\beta$ -sheet as well as in those parts of the N-terminal domain that can be assigned (again the flexible linker residues could not be assigned). This overlap in chemical shifts includes the Trp indole side chain NH resonance. There are large changes in chemical shifts at the loop where the M121E mutation occurs. There are smaller changes in chemical shifts of residues near this mutation site but also near the phenolic group of the chromophore consistent with the coexistence of distinct

patterns of H-bonding around the chromophore and Glu67 (Glu46 in wild-type numbering). Taken together, these data indicate that the M121E-cPYP mutant adopts much the same overall dark-state structure as cPYP except that the mutation alters the details of the H-bonding patterns near the chromophore. The same conclusion was reached by Sasaki et al. with regard to the dark-state structure of the M100L mutant of wtPYP<sup>41</sup> and by Devanathan et al. with regard to the M100A mutant.<sup>45</sup>

**Light-Driven Conformational Change of M121E-cPYP.** Joshi et al.<sup>40</sup> have shown that the photocycles undergone by both the protonated and deprotonated Y42F-PYP mutants are essentially the same. We therefore expected that, although the switching efficiency may be lower, the conformational changes that ensue should be unaffected by the presence of the intermediate spectral form in the M121E-cPYP construct.

To characterize the nature of the conformational change, we first measured the CD spectrum of M121E-cPYP after exposure to blue light (Figure 7a). Only a small change in the CD spectrum was observed. A similarly small CD change for wtPYP was seen by Lee et al.,<sup>46</sup> who interpreted this as indicating a molten globule-like state was formed upon irradiation in which secondary structural elements were preserved but tertiary contacts were lost. Interestingly, a larger CD change was seen by Sasaki et al.<sup>41</sup> in the M100L-PYP mutant. These authors suggested that the molten globule state was in equilibrium with a structure in which helical secondary structure had been lost. Because the N-terminal cap contains only short helical sections, its rearrangement may not lead to large changes in the overall secondary structure.

The  $^{15}\text{N}$ – $^1\text{H}$  HSQC spectrum of M121E-cPYP in dark-adapted and irradiated states (Figure 9) shows the changes expected on the basis of the wild-type protein with large changes in chemical shifts, an increase in signal intensity in the region of the spectrum associated with disordered structure, and a large decrease in the total number of peaks indicating extensive conformational exchange on a millisecond time scale.<sup>47–52</sup>

Numerous pieces of evidence have led to the conclusion that blue light irradiation of wtPYP leads to large-scale rearrangements and/or detachment of the N-terminal cap domain from the rest of the protein. These data include NMR studies of wtPYP and its mutants, H–D exchange measurements, DEER measurements, and, most recently, pump–probe X-ray solution



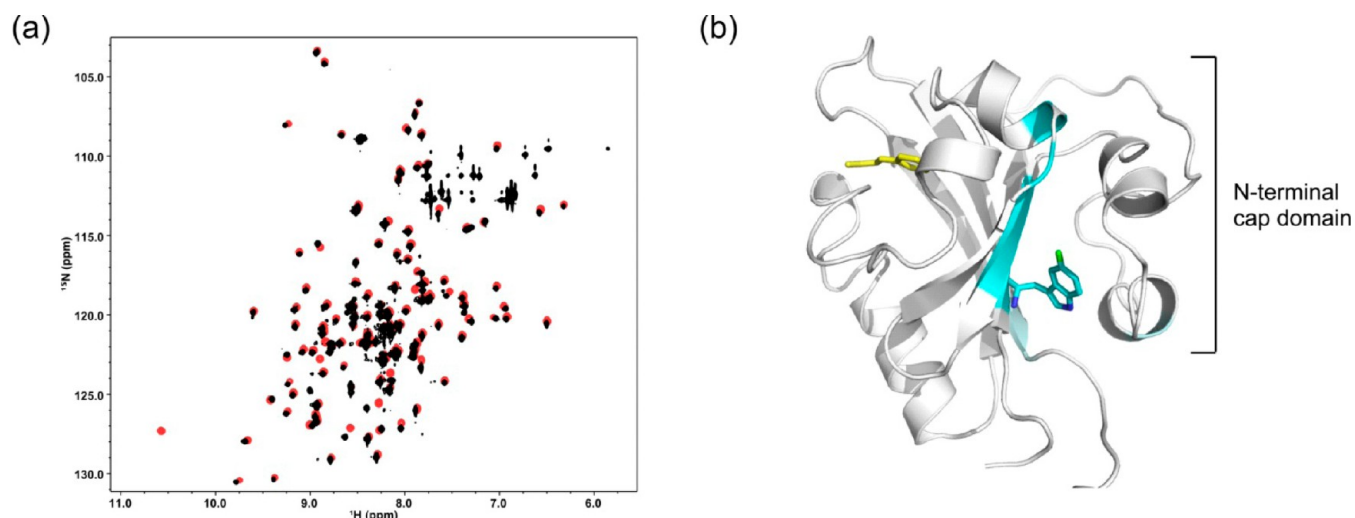


**Figure 10.** (a)  $^{15}\text{N}$ - $^1\text{H}$  HSQC spectra M121E-cPYP with (black) and without (red) incorporation of  $^{19}\text{F}$ Trp. (b) Chemical shifts showing perturbation are clustered in space around the fluorine atom (green) on the Trp indole side chain. This model was produced using PyMol.

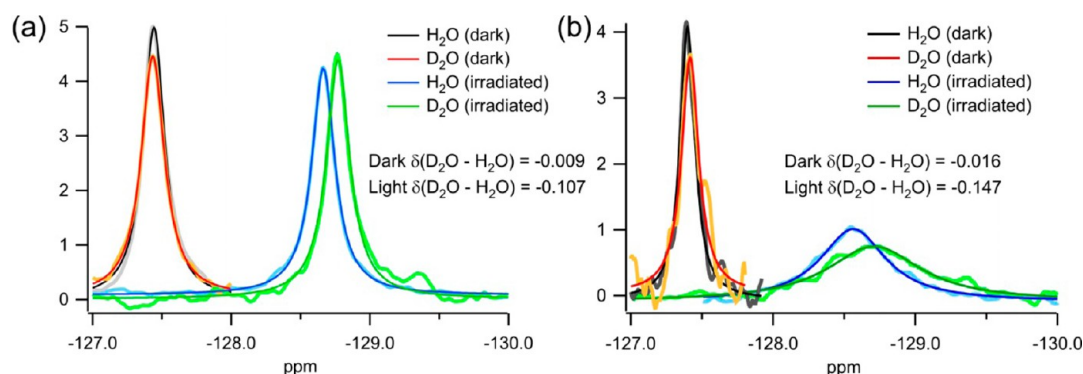


**Figure 11.**  $^{19}\text{F}$  spectra of 5F-Trp-labeled M100E-PYP (a) and M121E-cPYP (b) at 30 °C under the conditions indicated in the legend.

scattering data.<sup>17,20,49,50,53–55</sup> A central question in this study is whether the light-driven rearrangement of the N-terminal domain seen in the wild type also occurs in the M121E-cPYP construct.

To address this question directly, we opted to use the single Trp residue as a probe. As shown in Figure 10, Trp7 (residue 119 in wtPYP numbering) is buried in the dark-state structure (as calculated by Surface Racer<sup>56</sup>) as a consequence of packing of the N-terminal cap against the rest of the protein. If the N-terminal cap becomes detached or substantially reorganized, the Trp residue is expected to become solvent-exposed. Indeed, fluorescence measurements indicate this Trp residue becomes exposed in the light state of wtPYP and is completely solvent-exposed in the  $\Delta 25$  PYP mutant lacking the N-terminal cap.<sup>21,57</sup> Rather than using Trp fluorescence methods, which can be complicated by the transfer of energy to the chromophore in PYP,<sup>58</sup> we opted to use  $^{19}\text{F}$  NMR measurements of a  $^{19}\text{F}$ Trp-substituted analogue of M121E-cPYP.  $^{19}\text{F}$  NMR spectra of fluorinated proteins often reveal dramatic changes in chemical shifts and line shapes between different folded states.<sup>59</sup> Moreover, changing the solvent from  $\text{D}_2\text{O}$  for  $\text{H}_2\text{O}$  is known to yield an easily measured chemical shift perturbation of  $^{19}\text{F}$  nuclei that are solvent-exposed, thus providing a quantitative measure of the degree of solvent exposure of the  $^{19}\text{F}$ Trp site.<sup>28</sup>

We first measured the  $^{15}\text{N}$ - $^1\text{H}$  HSQC spectrum of  $^{19}\text{F}$ Trp-labeled M121E-cPYP and M100E-PYP to assess the degree of

structural perturbation introduced by the fluorine label. Figure 10a shows an overlay of this spectrum with that of the unlabeled protein for cPYP. Spectra for M100E-PYP are included in the Supporting Information. Chemical shift perturbations are mapped onto the modeled M121E-cPYP structure in Figure 10b. Only small changes are seen at sites close in space to the  $^{19}\text{F}$  atom, confirming the nonperturbing nature of this single-atom substitution. The HSQC data, together with UV-vis spectra and measurements of thermal relaxation rates (Supporting Information), indicate the fluorine substitution introduces minor local perturbations in the M100E-PYP protein also.

We then measured  $^{19}\text{F}$  NMR signals from the M100E-PYP and M121E-cPYP labeled proteins under both dark-state and irradiated conditions in both  $\text{H}_2\text{O}$  and  $\text{D}_2\text{O}$  at a series of temperatures. Figure 11 shows these data for 30 °C; lower and higher temperatures are included in the Supporting Information. The dark-adapted states of both M100E-PYP and M121E-cPYP gave sharp signals for the fluorine label near -127.4 ppm, and these showed very small solvent isotope shifts (<0.016 ppm) consistent with a buried location for the Trp residue. Under similar conditions, the solvent isotope shift  $\Delta\delta(\text{D}_2\text{O}-\text{H}_2\text{O})$  for 5F-Trp free in solution is -0.109 ppm.<sup>28</sup> At higher temperatures, the solvent isotope shifts became larger (see the Supporting Information), consistent with some temperature-induced loosening of the structure. Irradiation caused the  $^{19}\text{F}$  signals to move upfield for both M100E-PYP and M121E-cPYP

(Figure 11 and the Supporting Information), consistent with enhanced solvent exposure.<sup>28</sup> Irradiation also produced broadening of the <sup>19</sup>F signal, particularly for the circular permutant (Figure 11). The degree of broadening was highly temperature sensitive with light-state signals showing line widths (full width at half-maximum values) of 400 Hz at 20 °C and 130 Hz at 40 °C. This behavior is consistent with a large degree of conformational exchange of the Trp residue in the light state of M121E-cPYP.<sup>60</sup> The observation of large solvent isotope shifts,  $\Delta\delta(\text{D}_2\text{O}-\text{H}_2\text{O})$  (Figure 11 and the Supporting Information), for the <sup>19</sup>F signal upon irradiation provides direct evidence that the Trp indole side chain is highly exposed in the light state of both M100E-PYP and M121E-cPYP.

#### Prospects for Photocontrol of Target Sequences.

Overall, the data presented here are consistent with a picture in which M121E-cPYP adopts a well-folded dark state that is structurally very similar to that of wtPYP except for small perturbations in the N-terminal cap domain. Irradiation then causes a transition to a globally more flexible structure undergoing extensive conformational exchange in which the N-terminal cap that normally prevents solvent exposure of the Trp residue has moved to permit essentially complete solvent exposure. A picture of this light-driven conformational change is shown in Figure 12. The dark-state structure is modeled on

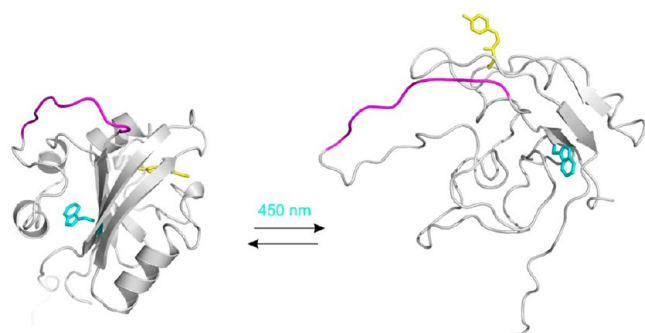


**Figure 12.** Models of dark-adapted (left) and blue light-irradiated (right) M121E-cPYP based on PDB entries 1NWZ<sup>36</sup> and 2KX6,<sup>20</sup> respectively. The insert sequence is colored magenta; the chromophore is shown as yellow sticks, and the Trp residue is shown as cyan sticks. These models were produced using PyMol.

that determined by X-ray diffraction of wtPYP (PDB entry 1NWZ) by Genick et al.<sup>36</sup> The light-state structure is based on a single structure taken from the ensemble of structures (PDB entry 2KX6) reported by Ramachandran et al. for the light state of wtPYP.<sup>20</sup> The GGSGGGSGG insert sequence is highlighted in each model. On the basis of the data described here, it is likely that the conformational dynamics of this insert and particularly its accessibility will be affected by the large changes occurring in PYP. On the basis of our previous experience with loop insertion, a wide range of peptide sequences and lengths are likely to be tolerated at this site.<sup>37,44</sup> Of course, inserts with defined conformational preferences may be coupled to PYP in a manner quite distinct from that of the short flexible linker studied here. It is unclear at present if the change in the N–C distance seen by Ramachandran et al.<sup>20</sup> would have an associated free energy change large enough to drive folding and/or unfolding of a given insert sequence. Nevertheless, the light-triggered conversion of the PYP domain to a globally flexible structure may permit uncovering of a binding surface or active site on an insert sequence even without the insert

undergoing a conformational change. We are currently exploring the effectiveness of circularly permuted PYP to serve as a scaffold for photoswitching a range of insert sequences.

## ■ ASSOCIATED CONTENT

### Supporting Information

Further spectroscopic details, including the pH dependence of UV–vis spectra of M121E-cPYP and characterization of M100E-PYP, <sup>19</sup>F spectra of 5F-Trp-labeled M121E-cPYP at a series of temperatures, and backbone NMR assignments of cPYP and M121E-cPYP. This material is available free of charge via the Internet at <http://pubs.acs.org>.

## ■ AUTHOR INFORMATION

### Corresponding Author

\*E-mail: [awoolley@chem.utoronto.ca](mailto:awoolley@chem.utoronto.ca). Telephone: (416) 978-0675. Fax: (416) 978-8775.

### Funding

This work has been supported by NSERC, CIHR, and National Institutes of Health Grant R01 MH086379. NMR instrumentation at the Centre for Spectroscopic Investigation of Complex Organic Molecules and Polymers was supported by the CFI (Project 19119) and the Ontario Research Fund.

### Notes

The authors declare no competing financial interest.

## ■ ACKNOWLEDGMENTS

We thank Prof. Scott Prosser for advice on fluorine NMR and Prof. Alan Davidson for use of his titrating fluorometer.

## ■ ADDITIONAL NOTE

<sup>a</sup>We use the term “light state” here to refer to the relatively long-lived putative signaling state of PYP. This state has also been called the I(2)’ state and the pB state.<sup>20</sup>

## ■ REFERENCES

- (1) Ha, J. H., and Loh, S. N. (2012) Protein conformational switches: From Nature to design. *Chem.—Eur. J.* 18, 7984–7999.
- (2) Strickland, D., Lin, Y., Wagner, E., Hope, C. M., Zayner, J., Antoniou, C., Sosnick, T. R., Weiss, E. L., and Glotzer, M. (2012) TULIPs: Tunable, light-controlled interacting protein tags for cell biology. *Nat. Methods* 9, 379–384.
- (3) Zhou, X. X., Chung, H. K., Lam, A. J., and Lin, M. Z. (2012) Optical control of protein activity by fluorescent protein domains. *Science* 338, 810–814.
- (4) Strickland, D., Yao, X., Gawlak, G., Rosen, M. K., Gardner, K. H., and Sosnick, T. R. (2010) Rationally improving LOV domain-based photoswitches. *Nat. Methods* 7, 623–626.
- (5) Airan, R. D., Thompson, K. R., Fenno, L. E., Bernstein, H., and Deisseroth, K. (2009) Temporally precise in vivo control of intracellular signalling. *Nature* 458, 1025–1029.
- (6) Wu, Y. I., Frey, D., Lungu, O. I., Jaehrig, A., Schlichting, I., Kuhlman, B., and Hahn, K. M. (2009) A genetically encoded photoactivatable Rac controls the motility of living cells. *Nature* 461, 104–108.
- (7) Lungu, O. I., Hallett, R. A., Choi, E. J., Aiken, M. J., Hahn, K. M., and Kuhlman, B. (2012) Designing photoswitchable peptides using the AsLOV2 domain. *Chem. Biol.* 19, 507–517.
- (8) Moglich, A., Ayers, R. A., and Moffat, K. (2010) Addition at the Molecular Level: Signal Integration in Designed Per-ARNT-Sim Receptor Proteins. *J. Mol. Biol.* 400, 477–486.
- (9) Moglich, A., and Moffat, K. (2010) Engineered photoreceptors as novel optogenetic tools. *Photochem. Photobiol. Sci.* 9, 1286–1300.

- (10) Christie, J. M., Gawthorne, J., Young, G., Fraser, N. J., and Roe, A. J. (2012) LOV to BLUF: Flavoprotein contributions to the optogenetic toolkit. *Mol. Plant* 5, 533–544.
- (11) Losi, A., and Gartner, W. (2011) Old chromophores, new photoactivation paradigms, trendy applications: Flavins in blue light-sensing photoreceptors. *Photochem. Photobiol.* 87, 491–510.
- (12) Woolley, G. A. (2012) Designing chimeric LOV photoswitches. *Chem. Biol.* 19, 441–442.
- (13) Nash, A. I., Ko, W. H., Harper, S. M., and Gardner, K. H. (2008) A conserved glutamine plays a central role in LOV domain signal transmission and its duration. *Biochemistry* 47, 13842–13849.
- (14) Harper, S. M., Neil, L. C., and Gardner, K. H. (2003) Structural basis of a phototropin light switch. *Science* 301, 1541–1544.
- (15) Kumauchi, M., Hara, M. T., Stalcup, P., Xie, A., and Hoff, W. D. (2008) Identification of six new photoactive yellow proteins: Diversity and structure-function relationships in a bacterial blue light photoreceptor. *Photochem. Photobiol.* 84, 956–969.
- (16) Lee, B. C., Pandit, A., Croonquist, P. A., and Hoff, W. D. (2001) Folding and signaling share the same pathway in a photoreceptor. *Proc. Natl. Acad. Sci. U.S.A.* 98, 9062–9067.
- (17) Hellingwerf, K. J., Hendriks, J., and Gensch, T. (2003) Photoactive Yellow Protein, a new type of photoreceptor protein: Will this “yellow lab” bring us where we want to go? *J. Phys. Chem. A* 107, 1082–1094.
- (18) Meyer, T. E., Kyndt, J. A., Memmi, S., Moser, T., Colon-Acevedo, B., Devreese, B., and Van Beeumen, J. J. (2012) The growing family of photoactive yellow proteins and their presumed functional roles. *Photochem. Photobiol. Sci.* 11, 1495–1514.
- (19) Kyndt, J. A., Vanrobaeys, F., Fitch, J. C., Devreese, B. V., Meyer, T. E., Cusanovich, M. A., and Van Beeumen, J. J. (2003) Heterologous production of *Halorhodospira halophila* holo-photoactive yellow protein through tandem expression of the postulated biosynthetic genes. *Biochemistry* 42, 965–970.
- (20) Ramachandran, P. L., Lovett, J. E., Carl, P. J., Cammarata, M., Lee, J. H., Jung, Y. O., Ihse, H., Timmel, C. R., and van Thor, J. J. (2011) The short-lived signaling state of the photoactive yellow protein photoreceptor revealed by combined structural probes. *J. Am. Chem. Soc.* 133, 9395–9404.
- (21) Morgan, S. A., Al-Abdul-Wahid, M. S., and Woolley, G. A. (2010) Structure-based design of a photocontrolled DNA binding protein. *J. Mol. Biol.* 399, 94–112.
- (22) Fan, H. Y., Morgan, S. A., Brechun, K. E., Chen, Y. Y., Jaikaran, A. S., and Woolley, G. A. (2011) Improving a designed photocontrolled DNA-binding protein. *Biochemistry* 50, 1226–1237.
- (23) Morgan, S. A., and Woolley, G. A. (2010) A photoswitchable DNA-binding protein based on a truncated GCN4-photoactive yellow protein chimera. *Photochem. Photobiol. Sci.* 9, 1320–1326.
- (24) Ui, M., Tanaka, Y., Araki, Y., Wada, T., Takei, T., Tsumoto, K., Endo, S., and Kinbara, K. (2012) Application of photoactive yellow protein as a photoresponsive module for controlling hemolytic activity of staphylococcal  $\alpha$ -hemolysin. *Chem. Commun.* 48, 4737–4739.
- (25) Devanathan, S., Genick, U. K., Getzoff, E. D., Meyer, T. E., Cusanovich, M. A., and Tollin, G. (1997) Preparation and properties of a 3,4-dihydroxycinnamic acid chromophore variant of the photoactive yellow protein. *Arch. Biochem. Biophys.* 340, 83–89.
- (26) Chagnenet-Barret, P., Espagne, A., Katsonis, N., Charier, S., Baudin, J. B., Jullien, L., Plaza, P., and Martin, M. M. (2002) Excited-state relaxation dynamics of a PYP chromophore model in solution: Influence of the thioester group. *Chem. Phys. Lett.* 365, 285–291.
- (27) Clarke, J., and Fersht, A. R. (1993) Engineered disulfide bonds as probes of the folding pathway of barnase: Increasing the stability of proteins against the rate of denaturation. *Biochemistry* 32, 4322–4329.
- (28) Evanics, F., Bezsonova, I., Marsh, J., Kiteviski, J. L., Forman-Kay, J. D., and Prosser, R. S. (2006) Tryptophan solvent exposure in folded and unfolded states of an SH3 domain by  $^{19}\text{F}$  and  $^1\text{H}$  NMR. *Biochemistry* 45, 14120–14128.
- (29) Ikura, M., Kay, L. E., and Bax, A. (1990) A novel approach for sequential assignment of  $^1\text{H}$ ,  $^{13}\text{C}$ , and  $^{15}\text{N}$  spectra of proteins: Heteronuclear triple-resonance three-dimensional NMR spectroscopy. Application to calmodulin. *Biochemistry* 29, 4659–4667.
- (30) Wittekind, M., and Mueller, L. (1993) HNCACB, a high-sensitivity 3D NMR experiment to correlate amide-proton and nitrogen resonances with the  $\alpha$ -carbon and  $\beta$ -carbon resonances in proteins. *J. Magn. Reson., Ser. B* 101, 201–205.
- (31) Grzesiek, S., and Bax, A. (1992) Correlating backbone amide and side-chain resonances in larger proteins by multiple relayed triple resonance NMR. *J. Am. Chem. Soc.* 114, 6291–6293.
- (32) Grzesiek, S., Anglister, J., and Bax, A. (1993) Correlation of backbone amide and aliphatic side-chain resonances in C-13/N-15-enriched proteins by isotropic mixing of C-13 magnetization. *J. Magn. Reson., Ser. B* 101, 114–119.
- (33) Mohebbi, A., and Shaka, A. J. (1991) Improvements in C-13 broad-band homonuclear cross-polarization for 2D and 3D NMR. *Chem. Phys. Lett.* 178, 374–378.
- (34) Delaglio, F., Grzesiek, S., Vuister, G. W., Zhu, G., Pfeifer, J., and Bax, A. (1995) NMRPipe: A multidimensional spectral processing system based on UNIX pipes. *J. Biomol. NMR* 6, 277–293.
- (35) Kanelis, V., Forman-Kay, J. D., and Kay, L. E. (2001) Multidimensional NMR methods for protein structure determination. *IUBMB Life* 52, 291–302.
- (36) Getzoff, E. D., Gutwin, K. N., and Genick, U. K. (2003) Anticipatory active-site motions and chromophore distortion prime photoreceptor PYP for light activation. *Nat. Struct. Biol.* 10, 663–668.
- (37) Butler, J. S., Mitrea, D. M., Mitrousis, G., Cingolani, G., and Loh, S. N. (2009) Structural and thermodynamic analysis of a conformationally strained circular permutant of barnase. *Biochemistry* 48, 3497–3507.
- (38) Pool, T. J., Oktaviani, N. A., Kamikubo, H., Kataoka, M., and Mulder, F. A. A. (2013) H-1, C-13, and N-15 resonance assignment of photoactive yellow protein. *Biomol. NMR Assignments* 7, 97–100.
- (39) Genick, U. K., Devanathan, S., Meyer, T. E., Canestrelli, I. L., Williams, E., Cusanovich, M. A., Tollin, G., and Getzoff, E. D. (1997) Active site mutants implicate key residues for control of color and light cycle kinetics of photoactive yellow protein. *Biochemistry* 36, 8–14.
- (40) Joshi, C. P., Otto, H., Hoersch, D., Meyer, T. E., Cusanovich, M. A., and Heyn, M. P. (2009) Strong hydrogen bond between glutamic acid 46 and chromophore leads to the intermediate spectral form and excited state proton transfer in the Y42F mutant of the photoreceptor photoactive yellow protein. *Biochemistry* 48, 9980–9993.
- (41) Sasaki, J., Kumauchi, M., Hamada, N., Oka, T., and Tokunaga, F. (2002) Light-induced unfolding of photoactive yellow protein mutant M100L. *Biochemistry* 41, 1915–1922.
- (42) Kumauchi, M., Hamada, N., Sasaki, J., and Tokunaga, F. (2002) A role of methionine 100 in facilitating PYP(M)-decay process in the photocycle of photoactive yellow protein. *J. Biochem.* 132, 205–210.
- (43) Szilagyi, A., Zhang, Y., and Zavodszky, P. (2012) Intra-chain 3D segment swapping spawns the evolution of new multidomain protein architectures. *J. Mol. Biol.* 415, 221–235.
- (44) Cutler, T. A., Mills, B. M., Lubin, D. J., Chong, L. T., and Loh, S. N. (2009) Effect of interdomain linker length on an antagonistic folding-unfolding equilibrium between two protein domains. *J. Mol. Biol.* 386, 854–868.
- (45) Devanathan, S., Genick, U. K., Canestrelli, I. L., Meyer, T. E., Cusanovich, M. A., Getzoff, E. D., and Tollin, G. (1998) New insights into the photocycle of *Ectothiorhodospira halophila* photoactive yellow protein: Photorecovery of the long-lived photobleached intermediate in the Met100Ala mutant. *Biochemistry* 37, 11563–11568.
- (46) Lee, B. C., Croonquist, P. A., Sosnick, T. R., and Hoff, W. D. (2001) PAS domain receptor photoactive yellow protein is converted to a molten globule state upon activation. *J. Biol. Chem.* 276, 20821–20823.
- (47) Fuentes, G., Nederveen, A. J., Kaptein, R., Boelens, R., and Bonvin, A. M. (2005) Describing partially unfolded states of proteins from sparse NMR data. *J. Biomol. NMR* 33, 175–186.
- (48) Bernard, C., Houben, K., Derix, N. M., Marks, D., van der Horst, M. A., Hellingwerf, K. J., Boelens, R., Kaptein, R., and van Nuland, N.



- A. (2005) The solution structure of a transient photoreceptor intermediate:  $\Delta 25$  photoactive yellow protein. *Structure* 13, 953–962.
- (49) Derix, N. M., Wechselberger, R. W., van der Horst, M. A., Hellingwerf, K. J., Boelens, R., Kaptein, R., and van Nuland, N. A. (2003) Lack of negative charge in the E46Q mutant of photoactive yellow protein prevents partial unfolding of the blue-shifted intermediate. *Biochemistry* 42, 14501–14506.
- (50) Craven, C. J., Derix, N. M., Hendriks, J., Boelens, R., Hellingwerf, K. J., and Kaptein, R. (2000) Probing the nature of the blue-shifted intermediate of photoactive yellow protein in solution by NMR: Hydrogen-deuterium exchange data and pH studies. *Biochemistry* 39, 14392–14399.
- (51) Dux, P., Rubinstenn, G., Vuister, G. W., Boelens, R., Mulder, F. A., Hard, K., Hoff, W. D., Kroon, A. R., Crielard, W., Hellingwerf, K. J., and Kaptein, R. (1998) Solution structure and backbone dynamics of the photoactive yellow protein. *Biochemistry* 37, 12689–12699.
- (52) Rubinstenn, G., Vuister, G. W., Mulder, F. A., Dux, P. E., Boelens, R., Hellingwerf, K. J., and Kaptein, R. (1998) Structural and dynamic changes of photoactive yellow protein during its photocycle in solution. *Nat. Struct. Biol.* 5, 568–570.
- (53) Khan, J. S., Imamoto, Y., Harigai, M., Kataoka, M., and Terazima, M. (2006) Conformational changes of PYP monitored by diffusion coefficient: Effect of N-terminal  $\alpha$ -helices. *Biophys. J.* 90, 3686–3693.
- (54) Cheng, G., Cusanovich, M. A., and Wysocki, V. H. (2006) Properties of the dark and signaling states of photoactive yellow protein probed by solution phase hydrogen/deuterium exchange and mass spectrometry. *Biochemistry* 45, 11744–11751.
- (55) Kim, T. W., Lee, J. H., Choi, J., Kim, K. H., van Wilderen, L. J., Guerin, L., Kim, Y., Jung, Y. O., Yang, C., Kim, J., Wulff, M., van Thor, J. J., and Ihse, H. (2012) Protein structural dynamics of photoactive yellow protein in solution revealed by pump-probe X-ray solution scattering. *J. Am. Chem. Soc.* 134, 3145–3153.
- (56) Tsodikov, O. V., Record, M. T., Jr., and Sergeev, Y. V. (2002) Novel computer program for fast exact calculation of accessible and molecular surface areas and average surface curvature. *J. Comput. Chem.* 23, 600–609.
- (57) Gensch, T., Hendriks, J., and Hellingwerf, K. J. (2004) Tryptophan fluorescence monitors structural changes accompanying signalling state formation in the photocycle of photoactive yellow protein. *Photochem. Photobiol. Sci.* 3, 531–536.
- (58) Hoersch, D., Otto, H., Cusanovich, M. A., and Heyn, M. P. (2008) Distinguishing chromophore structures of photocycle intermediates of the photoreceptor PYP by transient fluorescence and energy transfer. *J. Phys. Chem. B* 112, 9118–9125.
- (59) Danielson, M. A., and Falke, J. J. (1996) Use of  $^{19}\text{F}$  NMR to probe protein structure and conformational changes. *Annu. Rev. Biophys. Biomol. Struct.* 25, 163–195.
- (60) Hoeltzli, S. D., and Frieden, C. (1994)  $^{19}\text{F}$  NMR spectroscopy of  $[6\text{-}^{19}\text{F}]$ tryptophan-labeled *Escherichia coli* dihydrofolate reductase: Equilibrium folding and ligand binding studies. *Biochemistry* 33, 5502–5509.